ENSTA Bretagne · Ifremer
15ÈMES JOURNÉES DE L'HYDRODYNAMIQUE
22 - 24 novembre 2016 - Brest

AN INVESTIGATION OF THE RESONANT SLOSHING MOTION IN A RECTANGULAR TANK WITH MULTIPLE VERTICAL CYLINDERS

ÉTUDE THÉORIQUE ET EXPÉRIMENTALE DU BALLOTTEMENT DANS UNE CUVE RECTANGULAIRE REMPLIE DE CYLINDRES VERTICAUX

Bernard MOLIN, **Fabien REMY**

Aix Marseille Université, CNRS, Centrale Marseille, IRPHE UMR 7342, 13451 Marseille cedex 13
bernard.molin@centrale-marseille.fr, fabien.remy@centrale-marseille.fr

Summary

Sloshing tests are performed with a rectangular tank filled with a large number of vertical cylinders, in a regular arrangement. The cylinders are bottom-mounted and run through the free surface. The tank is harmonically oscillated in surge at frequencies around the natural frequency of the first sloshing mode. The free surface elevation at the tank end and the hydrodynamic loads are measured. The experimental RAOs of the free surface elevation are compared with numerical values obtained from idealizing the cylinder cluster as an anisotropic porous medium, and following a modal approach. Quadratic damping terms are introduced in the modal equations to account for energy dissipation due to flow separation at the cylinders. Experimental and numerical values of the damping coefficient are also compared. Good agreement is obtained.

Résumé

Des essais de ballottement sont effectués avec une cuve rectangulaire remplie d'un grand nombre de cylindres verticaux. Les cylindres sont fixés au fond et percent la surface libre. Le cuve est soumise à des mouvements de translation, à des fréquences voisines de la fréquence propre du premier mode de ballottement. Les mesures consistent en l'élévation de surface libre (à la paroi) et les efforts hydrodynamiques. Un modèle théorique est proposé où la cuve est assimilée à milieu poreux anisotrope, et où une approche modale est appliquée pour représenter le ballottement. Un amortissement quadratique est introduit dans les équations modales pour exprimer la dissipation d'énergie due aux effets visqueux sur les cylindres. Un bon accord est obtenu entre essais et calculs, pour la fonction de transfert de l'élévation de surface libre, et pour l'amortissement hydrodynamique.

1 Introduction

There has been a strong interest, in coastal engineering, for wave transformation and decay through interaction with marine vegetation like seaweed, kelp or coral canopies. In experiments and numerical models these obstacles are often idealized as regular arrays of vertical cylinders (e.g. see Lowe *et al.* 2005, Augustin *et al.* 2009, Mei *et al.* 2011). A thorough review can be found in Chen *et al.* (2016). Recently further investigations, reported in Arnaud *et al.* (2016), have been performed at Seatech in Toulon. In all of these experiments the cylinder diameters are small compared with the wavelengths, typically of the order of 1 %.

When waves propagate through such dense arrays of vertical cylinders they decay in amplitude, as a result of friction and flow separation, but they also undergo other modifications like partial reflection and shortening of the wavelength. To describe these phenomena numerically different routes have been followed. One approach is to consider the cylinder array as an homogeneous porous medium and to introduce into the Bernoulli equation extra inertial and dissipative terms, still relying on potential flow theory (Sollitt & Cross 1972, Yu & Chwang 1994). When dissipative effects are discarded this leads to the following dispersion equation

$$\omega^2 S = g\, k\ \tanh kh \tag{1}$$

with ω the angular frequency, k the wavenumber, h the waterdepth and $S = 1 + C_m\,(1-\tau)/\tau$, C_m an added mass coefficient and τ the porosity (water volume divided by total volume).

In Molin *et al.* (2016) some experiments are reported which were undertaken to verify the applicability of this dispersion equation. These experiments did not consist in running regular waves through cylinder arrays in a canal, alike in Arnaud *et al.* (2016), but in sloshing tests: a rectangular tank filled with vertical cylinders is undergoing forced horizontal motion around the natural frequency of the first sloshing mode. When resonance is attained it means that the oscillation frequency and twice the length of the tank are linked by the dispersion equation.

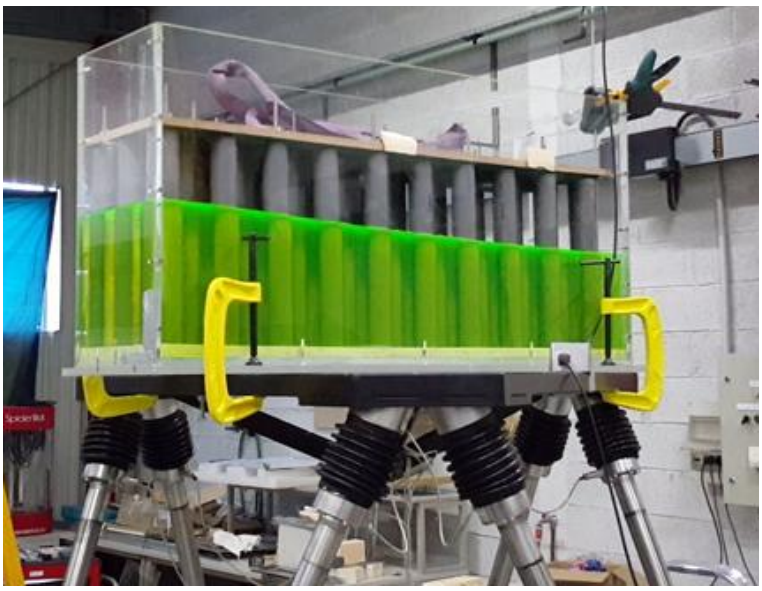

Figure 1: The tank on the Hexapode.

Figure 1 shows the experimental set-up: the tank is 1.2 m long, 0.3 m wide, the waterheight is 0.235 m (alike in the Seatech experiments). Different cylinder diameters were tested (2 cm, 3.2 cm, 5 cm) and different porosities, from about 70 % up to 90 % through varying the number of cylinders,

in a staggered arrangement. Both the emerging case and the fully submerged case (with different cylinder heights) were covered.

The dispersion equation derived from these experiments was compared with equation (1) and with other approaches based on linearized potential flow theory, accounting individually for all cylinders. It was found that none of them worked really well and a new approach was proposed, where one considers the fluid domain to be anisotropic, and starts from writing the linearized Euler equations as

$$S\,U_t = -\frac{1}{\rho}\,p_x \tag{2}$$

$$S\,V_t = -\frac{1}{\rho}\,p_y \tag{3}$$

$$W_t = -\frac{1}{\rho}\,p_z - g\,z \tag{4}$$

$$U_x + V_y + W_z = 0 \tag{5}$$

with the S coefficient only in the horizontal momentum equations, at variance with previous investigations. Then the following dispersion equation was obtained

$$\omega^2\,\sqrt{S} = g\,k\,\tanh\left(kh/\sqrt{S}\right), \tag{6}$$

and turned out to provide the best fit with the experiments (with $C_m = 1$, as expected for circular cylinders).

In this paper we use results from the same experiments as in Molin *et al.* (2016) and we aim at calculating the sloshing response in the tank. We adopt the same starting equations as just written above. Then we follow a modal approach similar to the method presented in Molin *et al.* (2002) where linearized potential flow theory is used and the dissipative effects due to viscous effects are introduced as linear and quadratic damping terms in the modal equations. Because of space limitations only the emerging case at the intermediate diameter (3.2 cm) is considered.

2 Theoretical model

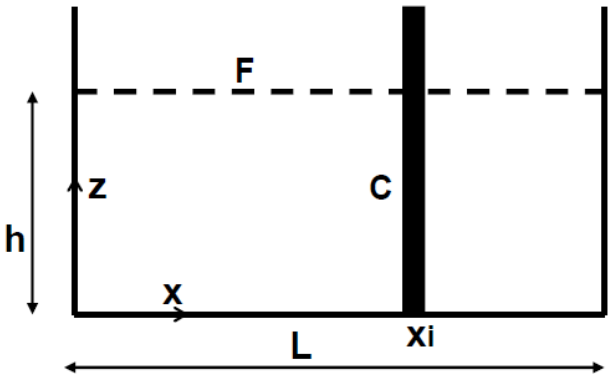

Figure 2: Geometry.

Figure 2 shows the geometry of the problem. The length of the tank is L, its width is B, the waterheight is h, the coordinate system (x, y, z) has its origin at a bottom left corner. The tank is

filled with vertical cylinders going through the free surface, only one of them being shown in the figure.

From equations (2), (3), (4), through differentiations, we get

$$\frac{\partial}{\partial t}(U_y - V_x) = \frac{\partial}{\partial t}(S\,U_z - W_x) = \frac{\partial}{\partial t}(S\,V_z - W_y) = 0 \tag{7}$$

These conditions can be fulfilled a priori if we introduce a "velocity potential" $\Phi(x, y, z, t)$ such that

$$U = \frac{\Phi_x}{S} \qquad V = \frac{\Phi_y}{S} \qquad W = \Phi_z \tag{8}$$

Mass conservation then gives the modified Laplace equation

$$\Phi_{xx} + \Phi_{yy} + S\,\Phi_{zz} = 0 \tag{9}$$

The usual linearized Bernoulli-Lagrange equation is recovered for the pressure:

$$p = p_0 - \rho\,g\,z - \rho\,\Phi_t \tag{10}$$

so that the usual free surface equation still applies

$$g\,\Phi_z + \Phi_{tt} = 0 \tag{11}$$

At some stage we will need to apply Green's identity which holds if the velocity potential verifies the actual Laplace equation. So we introduce a stretched vertical coordinate $\zeta = z/\sqrt{S} = z\,\sqrt{\tau}$ (we take $C_m \equiv 1$) so that $\Phi_{xx} + \Phi_{yy} + \Phi_{\zeta\zeta} = 0$.

Velocity potentials of the natural sloshing modes have the form

$$\Phi_n(x, \zeta, t) = \frac{A_n\,g}{\omega_n}\,\frac{\cosh\lambda_n\zeta}{\cosh\lambda_n\widetilde{h}}\,\cos\lambda_n x\,\sin(\omega_n t + \theta_n) \tag{12}$$

with $\lambda_n = n\,\pi/L$, L the length of the tank, $\widetilde{h} = h\,\sqrt{\tau}$ and the natural frequencies ω_n obtained from

$$\omega_n^2 = g\,\lambda_n\,\sqrt{\tau}\,\tanh\left(\lambda_n\,h\,\sqrt{\tau}\right) \tag{13}$$

To calculate the sloshing response of the tank under forced horizontal motion we follow closely the method of Molin *et al.* (2002) — see also Molin *et al.* (2003) — based on a modal decomposition.

We consider the tank undergoing a forced horizontal motion $X(t) = X_0\,\sin\omega t$. We write the velocity potential as

$$\Phi(x, y, \zeta, t) = \frac{X_0\,\omega}{\tau}\,\varphi(x, y, \zeta)\,\cos\omega t \tag{14}$$

The velocity potential $\varphi(x, y, \zeta)$ verifies the Laplace equation, the no-flow conditions $\partial\varphi/\partial\zeta = \varphi_\zeta = 0$ at the bottom ($\zeta = 0$), $\partial\varphi/\partial x = 1$ at the vertical walls ($x = 0$ and $x = L$), $\partial\varphi/\partial n = N_1 = -\cos\theta$ on the cylinders, and the free surface condition $g\,\sqrt{\tau}\,\varphi_\zeta - \omega^2\,\varphi = 0$ at $\zeta = \widetilde{h} = h\,\sqrt{\tau}$.

As in Molin *et al.* (2002) we decompose φ as $\varphi = \widetilde{\varphi} + \psi$ where $\widetilde{\varphi}$ is the infinite frequency potential that verifies $\widetilde{\varphi} = 0$ on the free surface and the no-flow conditions given above. The additional potential ψ verifies the homogeneous Neumann condition at all solid boundaries and the following free surface condition:

$$g\,\psi_\zeta\,\sqrt{\tau} - \omega^2\,\psi = -g\,\widetilde{\varphi}_\zeta\,\sqrt{\tau} \tag{15}$$

ψ can be written as a linear combination of natural modes:

$$\psi = \sum_{n=1}^{\infty} C_n\,\varphi_n = \sum_{n=1}^{\infty} C_n\,\frac{g}{\omega_n}\,\frac{\cosh\lambda_n\zeta}{\cosh\lambda_n\widetilde{h}}\,\cos\lambda_n x \tag{16}$$

From the free surface condition (15) the C_n coefficients are obtained as

$$C_n = -\frac{g\sqrt{\tau}}{\omega_n^2 - \omega^2} \frac{\int_F \widetilde{\varphi}_\zeta \, \varphi_n \, \mathrm{d}S}{\int_F \varphi_n^2 \, \mathrm{d}S} = \frac{g\sqrt{\tau}}{\omega_n^2 - \omega^2} \frac{\int_{S \cup C} \varphi_n \, N_1 \, \mathrm{d}S}{\int_F \varphi_n^2 \, \mathrm{d}S} \tag{17}$$

with F the free surface, S the tank walls, C the cylinders and N_1 the x-component of the normal vector outward the fluid domain. Green's identity has been used to transform the numerator, alike in Molin *et al.* (2002).

The modal potentials φ_n, as given in equation (16), do not fulfill the no-flow condition at the cylinders walls. Equation (16) can be viewed as an outer expansion. In the vicinity of a cylinder located in x_i, a better approximation of the modal potential φ_n is

$$\varphi_n(R, \theta, \zeta) \simeq \frac{g}{\omega_n} \frac{\cosh \lambda_n \zeta}{\cosh \lambda_n \widetilde{h}} \left[\cos \lambda_n x_i - \lambda_n \, \sin \lambda_n x_i \left(R + \frac{a^2}{R} \right) \cos \theta \right] \tag{18}$$

with a the cylinder radius and (R, θ, ζ) a local cylindrical coordinate system.

The integration of $\varphi_n \, N_1 = -\varphi_n \cos \theta$ over the cylinder wall gives

$$\int_{c_i} \varphi_n \, N_1 \, \mathrm{d}S = 2 \, \pi \, a^2 \, \frac{g}{\omega_n} \tanh \lambda_n \widetilde{h} \, \sin \lambda_n x_i \tag{19}$$

Summing up over all cylinders, assumed to be regularly located in the tank, one gets

$$\int_{\sum c_i} \varphi_n \, N_1 \, \mathrm{d}S = 4 \, (1 - \tau) \, \frac{g}{\omega_n} \frac{B \, L}{n \, \pi} \, \tanh \lambda_n \widetilde{h} \tag{20}$$

The integration over the two vertical walls at $x = 0$ and $x = L$ gives

$$\int_W \varphi_n \, N_1 \, \mathrm{d}S = -2 \, \frac{g}{\omega_n} \frac{B \, L}{n \, \pi} \, \tanh \lambda_n \widetilde{h} \tag{21}$$

The denominator in (17) is taken as

$$\int_F \varphi_n^2 \, \mathrm{d}S \simeq \frac{B \, L \, \tau \, g^2}{2 \, \omega_n^2} \tag{22}$$

so that

$$C_n \simeq -4 \, \frac{g\sqrt{\tau}}{\omega_n^2 - \omega^2} \, \frac{\omega_n}{g} \, \frac{\tanh \lambda_n \widetilde{h}}{n \, \pi} \, \frac{1 - 2 \, (1 - \tau)}{\tau} \tag{23}$$

Finally (again see Molin *et al.* 2002) it is obtained that the modal amplitudes A_n verify the pendulum equations

$$\ddot{A}_n + B_{1n} \, \dot{A}_n + B_{2n} \, \dot{A}_n \, |\dot{A}_n| + \omega_n^2 \, A_n = D_n \, \ddot{X}(t) \tag{24}$$

where extra damping terms have been introduced (B_{1n} a linear damping term due to friction, B_{2n} a quadratic damping term due to separation), and the D_n coefficient is given by

$$D_n = \frac{4 \, \tanh \lambda_n \widetilde{h}}{n \, \pi \, \sqrt{\tau}} \, \frac{1 - 2 \, (1 - \tau)}{\tau} \tag{25}$$

The experimental RAOs show a significative shift of the peak frequency as the sloshing amplitude increases. This wellknown feature is due to nonlinear (third-order) free surface effects (e.g. see Faltinsen & Timokha, 2009). To represent this shifting behavior, the mass-spring equation (24) for $n = 1$ is complemented with a cubic restoring term, as

$$\ddot{A}_1 + B_{11} \, \dot{A}_1 + B_{21} \, \dot{A}_1 \, |\dot{A}_1| + \omega_1^2 \, (1 + \alpha \, \lambda_1^2 \, A_1^2) \, A_1 = D_1 \, \ddot{X}(t) \tag{26}$$

For a clean tank (without cylinders inside) the theoretical α value is around 2.4 (see Appendix). Much higher values turned out to be needed in order to fit numerical and experimental RAOs, with the α value increasing with the number of cylinders in the tank. Presumably this is associated with increasing perturbations of the free surface.

In Molin *et al.* (2002) dissipation is considered to be due to friction and/or separation at the smooth/corrugated walls of the tank. Here friction at the wall is expected to play a negligible role as compared to separation at the cylinders. So we assume the B_{1n} coefficients to be nil and we follow an approach similar with the Appendix in Molin *et al.* (2002) to express the B_{21} coefficient for the first sloshing mode $n = 1$ which is the only one that needs to be damped given the explored range of frequencies.

To express the B_{21} coefficient, we assume that only the first sloshing mode is present in the tank, with the free surface elevation η and velocity potential Φ given by

$$\eta(x,t) = A \cos\lambda_1 x \ \cos\omega_1 t \tag{27}$$

$$\Phi(x,z,t) = -\frac{A\,g}{\omega_1}\,\frac{\cosh\lambda_1 z\sqrt{\tau}}{\cosh\lambda_1 h\sqrt{\tau}}\,\cos\lambda_1 x \ \sin\omega_1 t \tag{28}$$

Consider one vertical cylinder in $x = x_i$ with diameter D. The drag force is obtained from

$$\mathrm{d}F_D = \frac{1}{2}\,\rho\,C_D\,D\,\tau^2\,A^2\,\omega_1^2\,\sin\lambda_1 x_i\,|\sin\lambda_1 x_i|\,\frac{\cosh^2\lambda_1 z\sqrt{\tau}}{\sinh^2\lambda_1 h\sqrt{\tau}}\,\sin\omega_1 t\,|\sin\omega_1 t|\,\mathrm{d}z \tag{29}$$

Multiplying with the horizontal velocity, and integrating in z from 0 to h, then in time, one obtains the energy dissipated over one period as

$$\Delta E_1 = \frac{4}{9}\,\rho\,C_D\,D\,\tau^{3/2}\,A^3\,g\,\tanh\lambda_1 h\sqrt{\tau}\,|\sin\lambda_1 x_i|^3\,\left(1+\frac{3}{\sinh^2\lambda_1 h\sqrt{\tau}}\right) \tag{30}$$

Summing up over all cylinders assumed to be regularly set over the length of the tank gives the total dissipated energy:

$$\Delta E_1 = \frac{64}{27\,\pi^2}\,(1-\tau)\,\rho\,C_D\,\frac{B\,L}{D}\,\tau^{3/2}\,A^3\,g\,\tanh\lambda_1 h\sqrt{\tau}\,\left(1+\frac{3}{\sinh^2\lambda_1 h\sqrt{\tau}}\right) \tag{31}$$

The kinetic plus potential energy of the sloshing mode is taken to be

$$E_1 = \frac{1}{4}\,\rho\,g\,\tau\,A^2\,B\,L \tag{32}$$

So the relative energy dissipated over one period is:

$$\frac{\Delta E_1}{E_1} = \frac{256}{27\,\pi^2}\,(1-\tau)\,\sqrt{\tau}\,C_D\,\frac{A}{D}\,\tanh\lambda_1 h\sqrt{\tau}\,\left(1+\frac{3}{\sinh^2\lambda_1 h\sqrt{\tau}}\right) \tag{33}$$

For the modal oscillator the relative "energy" dissipated over one period is $16/3\,B_{21}\,A$. Identification with the previous expression gives the B_{21} value:

$$B_{21} = \frac{16}{9\,\pi^2}\,(1-\tau)\,\sqrt{\tau}\,\frac{C_D}{D}\,\tanh\lambda_1 h\sqrt{\tau}\,\left(1+\frac{3}{\sinh^2\lambda_1 h\sqrt{\tau}}\right) \tag{34}$$

The C_D value to use depends both on the β number $\beta = D^2/(\nu T)$ (ν the kinematic viscosity and T the period) and on the Keulegan-Carpenter number $K_C = 2\,\pi\,A/D$ (Sarpkaya, 2010). Here we only consider the tests with the emerging 3.2 cm diameter cylinders, so that the β value at resonance is around 600 and the K_C range is from $K_C \simeq 2$ (for $X_0 = 1$ mm) up to $K_C \simeq 6$ (for $X_0 = 1$ cm).

Some experimental information on the drag and added mass coefficients at relevant K_C and nearby β values ($\beta = 1035$) can be found in Sarpkaya (1986). These coefficients were derived from tests in a U-tube where quasi planar uniform flows can be achieved. In our sloshing tests, the flow is also quasi uniform by mid-tank where most of energy dissipation takes place: the vertical component of the flow velocity is nil and, due to the relatively shallow water condition, the horizontal velocity component varies by only 20 %from bottom to free surface. However Sarpkaya's experiments are for one isolated cylinder. From Sarpkaya's results it can be inferred that the range of drag coefficients is from 0.8 up to 2.0 as K_C increases from 2 up to 6.

3 Comparisons between numerical and experimental results

The table below shows the cylinder configurations that were tested and the porosities achieved. Here the porosity is defined as $\tau = 1 - N\,\pi a^2/(BL)$ with N the number of cylinders. Also shown in the table are the resonant frequencies (in rad/s) of the first sloshing mode, obtained in the experiments, and from applying the dispersion equation (6). The experimental value is taken as the position of the RAO peak at the lowest motion amplitude.

Number of cylinders	Porosity	ω_1 (exp)	ω_1 (num)
120	0.732	3.30	3.26
84	0.812	3.40	3.41
60	0.866	3.50	3.52
48	0.893	3.55	3.56

Good agreement can be observed between the experimental and theoretical values of the natural frequencies.

In each configuration the tank was oscillated at angular frequencies from 2.8 rad/s up to 4.2 rad/s, around the first sloshing mode, and amplitudes of 1 mm, 2 mm, 5 mm and 10 mm. The free surface elevation was measured at one end of the tank with a resistive gauge. Thanks to force sensors incorporated in the Hexapode the hydrodynamic loads were also obtained. Fourier analysis was then applied to the measurements to yield the RAO of the free surface elevation and the hydrodynamic coefficients of the tank, following

$$F_x(t) = \Re\left\{\mathrm{i}\ \rho\ X_0\ \omega^2\ L\,B\,h\ (C_a + \mathrm{i}\ C_b)\ \mathrm{e}^{-\mathrm{i}\,\omega\,t}\right\} \tag{35}$$

with $X(t) = X_0\,\sin\omega t$ the imposed motion, C_a the added mass coefficient and C_b the damping coefficient (see Molin & Remy 2013). The damping coefficient curves, alike the free surface elevation RAOs, show peaks at the natural frequency of the first sloshing mode.

In the calculations the drag coefficient C_D and the detuning coefficient α were adjusted in order to get the best fit between experimental and numerical RAOs of the free surface elevation. Even though it has been argued that C_D should depend on the Keulegan-Carpenter number, for the sake of simplicity the same value was used for all imposed motion amplitudes in the considered range (from 1 mm to 10 mm). Obviously better fits could be obtained by adjusting the C_D value on a case by case basis.

Results for the RAOs are given in Figures 3 through 6 for decreasing porosities, that is increasing number of cylinders, from 48 up to 120. The C_D and α values used are given in the captions. It can be observed that, as the number of cylinders increases, the C_D values decrease (from 2.2 down to 1.2) and the α values increase (from 12 up to 26). In the Appendix it is shown that the reference α value, for a clean tank (without cylinders), is about 2.4. It makes sense that an increasing number of cylinders enhances free surface nonlinearities. Why the drag coefficient needs to be decreased is less clear.

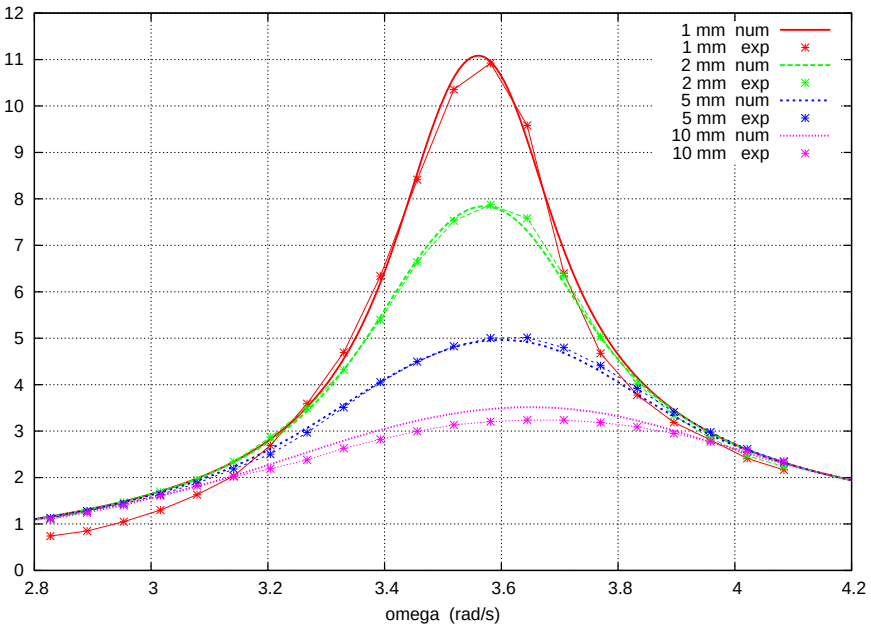

Figure 3: Porosity 89 %. $C_D = 2.2$, $\alpha = 12$. Numerical and experimental RAOs of the free surface elevation at the wall.

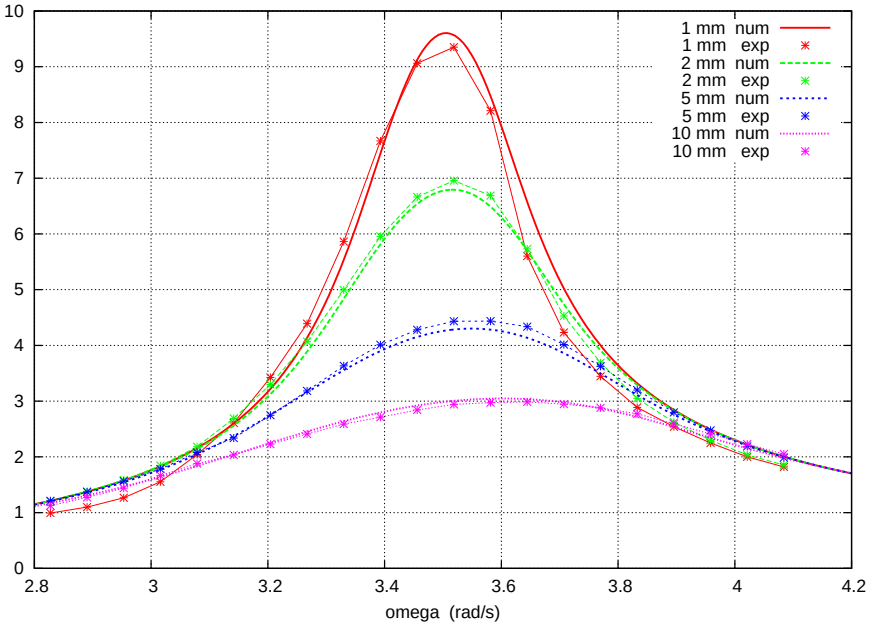

Figure 4: Porosity 86 %. $C_D = 2.2$, $\alpha = 18$. Numerical and experimental RAOs of the free surface elevation at the wall.

With the C_D and α coefficients properly adjusted the agreement between the experimental and numerical RAOs of the free surface elevation appears to be rather good in all porosity cases.

Figures 7 through 10 show the damping coefficient C_b as obtained experimentally from the measured force (see equation (35)) and numerically from the expression (31). The agreement is good at

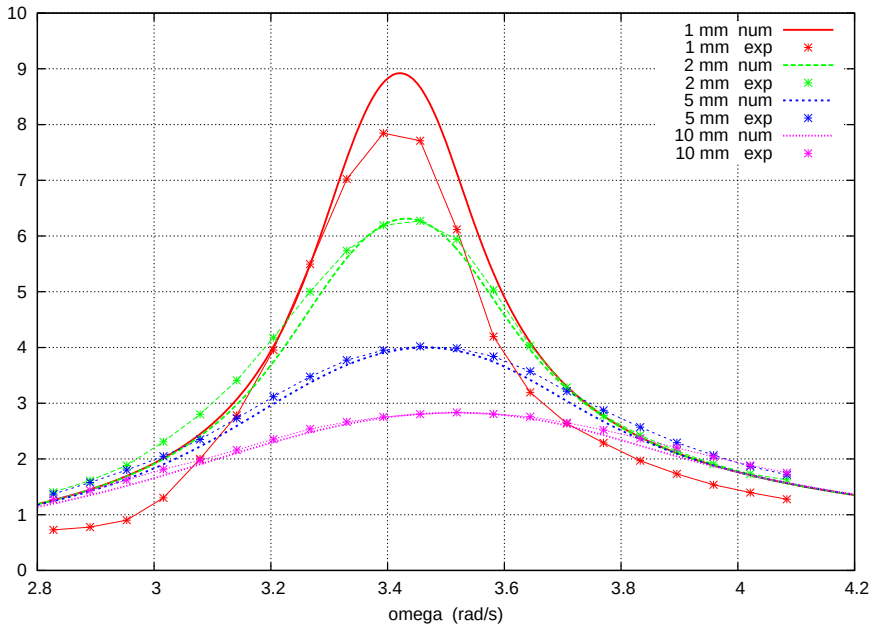

Figure 5: Porosity 80 %. $C_D = 1.6$, $\alpha = 20$. Numerical and experimental RAOs of the free surface elevation at the wall.

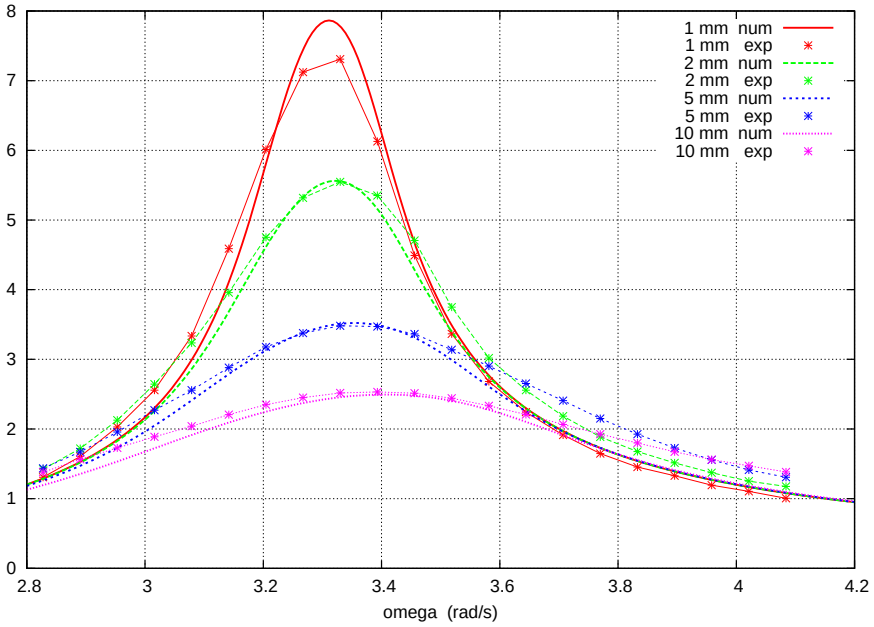

Figure 6: Porosity 72 %. $C_D = 1.2$, $\alpha = 26$. Numerical and experimental RAOs of the free surface elevation at the wall.

high porosities but degrades as the porosity decreases.

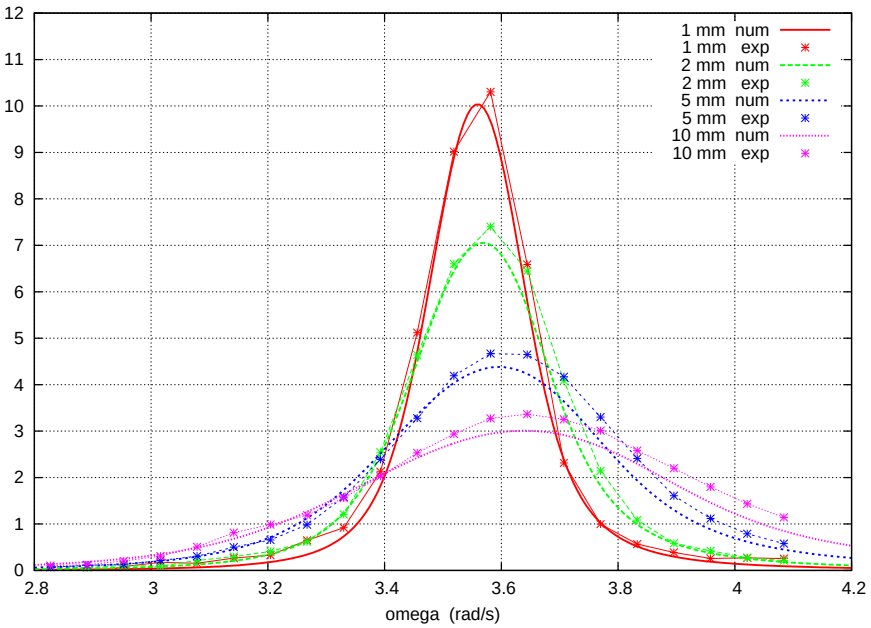

Figure 7: Porosity 89 %. $C_D = 2.2$, $\alpha = 12$. Damping coefficient.

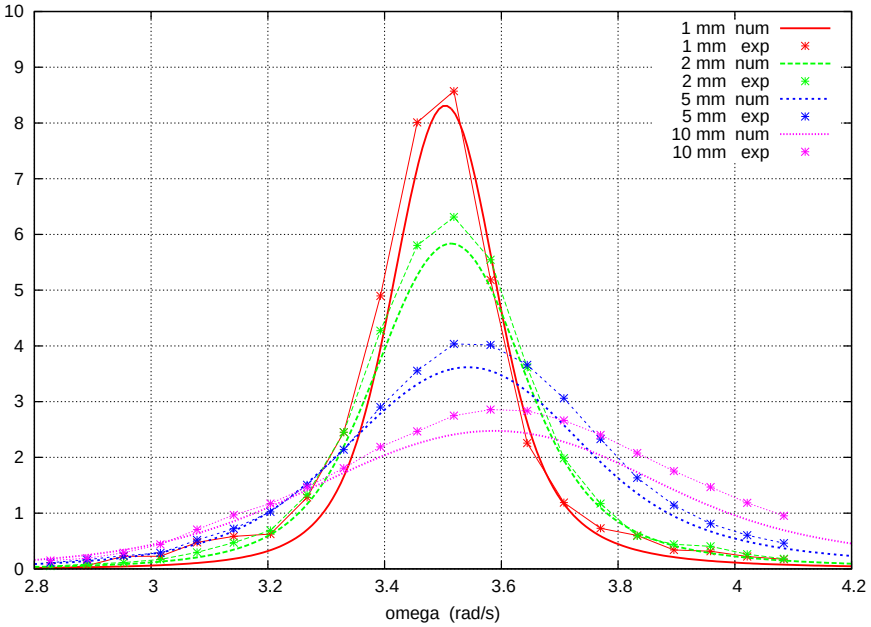

Figure 8: Porosity 86 %. $C_D = 2.2$, $\alpha = 18$. Damping coefficient.

4 Concluding remarks

In this paper we have proposed a semi-analytical approach to model wave interaction with dense arrays of vertical cylinders. Our approach combines some kind of linearized potential flow approach where viscous flow effects (drag) are introduced a posteriori as in the Morison equation. By "some kind of potential flow approach" we mean that a vertical stretching is introduced to account for added inertia effects due to the presence of the cylinders.

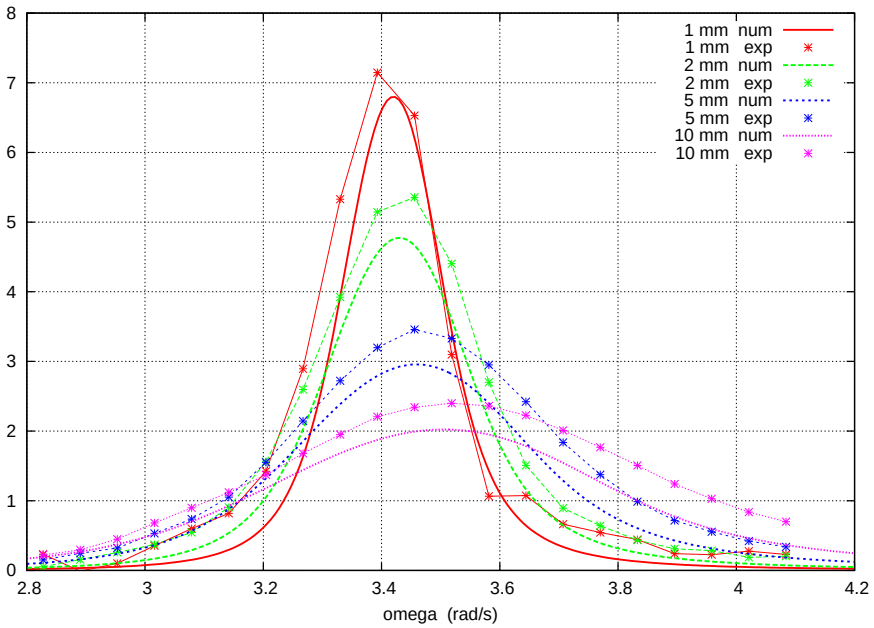

Figure 9: Porosity 80 %. $C_D = 1.6$, $\alpha = 20$. Damping coefficient.

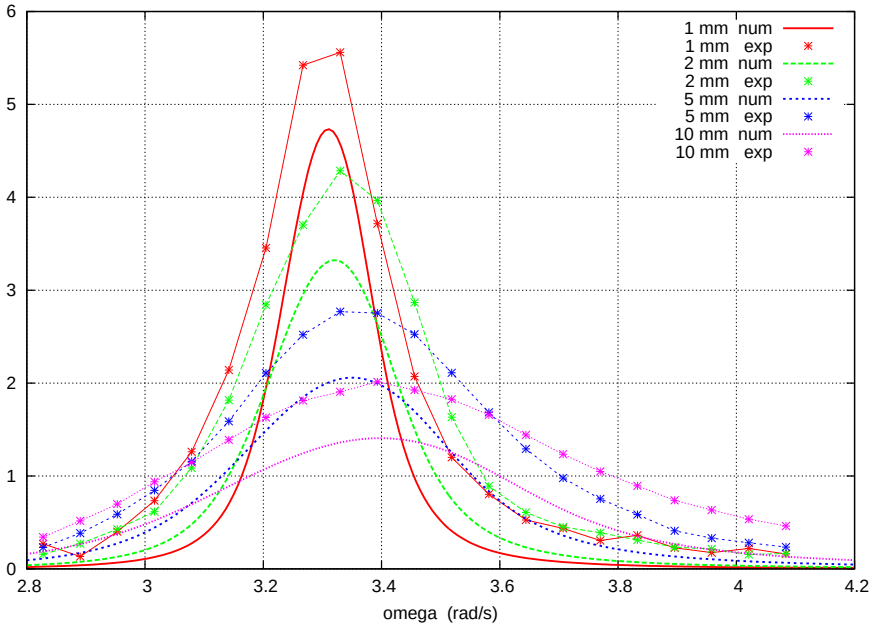

Figure 10: Porosity 72 %. $C_D = 1.2$, $\alpha = 26$. Damping coefficient.

With a proper tuning of the drag coefficient we have obtained a rather good agreement fo the RAO of the sloshing motion, in all porosity cases. It must be emphasized here that the porosity cases that we have considered are much lower than the reported cases in literature which are mostly in the range [0.95 1.0]. Many authors have relied on CFD models based on the Navier-Stokes equations (e.g. see Wu *et al.* 2013, Mei *et al.* 2014, Chen *et al.* 2016). Here we show that simpler ways can provide good numerical results.

A Shift of the natural frequency

It is known that, as the sloshing motion amplitude of the first mode increases, the peak frequency shifts to larger or smaller values, depending on the $\lambda_1 h$ value. The relative shift is given by

$$\frac{\Delta\omega}{\omega} = -\frac{1}{8}\,\lambda_1^2 A^2\,\tanh\lambda_1 h\,[f(\lambda_1 h, \lambda_1 h, \pi) + f(\lambda_1 h, \lambda_1 h, 0)/2] \tag{36}$$

where f is the interaction function given, for instance, in the Appendix of Molin *et al.* (2014). The quantity $\beta = f(\lambda_1 h, \lambda_1 h, \pi) + f(\lambda_1 h, \lambda_1 h, 0)/2$ is plotted in Figure 11

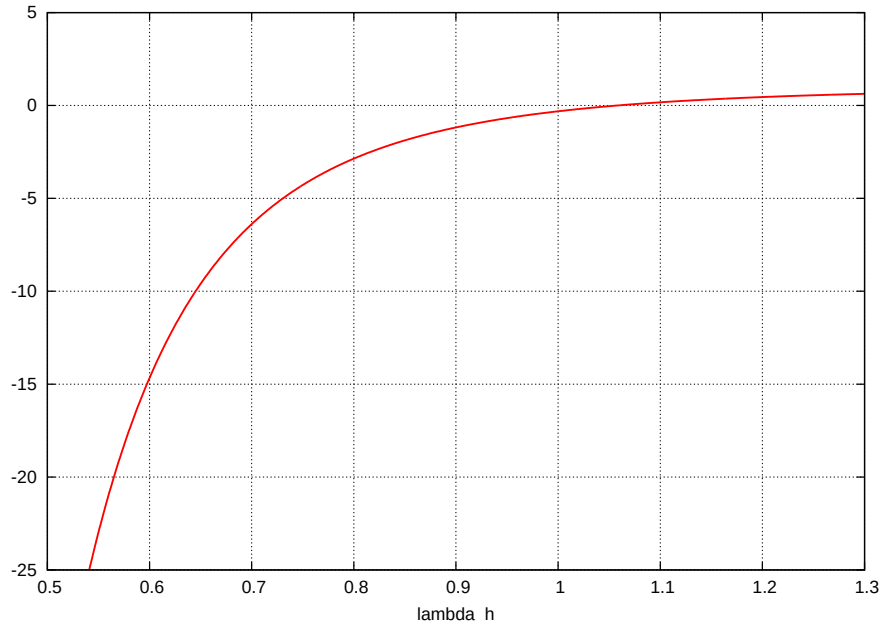

Figure 11: Function β vs λh.

When $\lambda_1 h$ is less than 1.058 (that is h/L less than 0.3368), the coefficient β is negative, meaning that the peak frequency increases when the amplitude increases (hard system). At $\lambda_1 h = 0.615$ the β value is -12.86.

The coefficient α in our Duffing oscillator (26) can be related to β. The resonant frequency is obtained from

$$-\omega^2 + \omega_1^2\left(1 + \frac{3}{4}\,\alpha\,\lambda_1^2\,A_{10}^2\right) = 0 \tag{37}$$

where A_{10} is the modal amplitude. This means

$$\frac{\Delta\omega_1}{\omega} = \frac{3}{8}\,\alpha\,\lambda_1^2\,A_{10}^2 \tag{38}$$

The reference value of α is therefore $\alpha = 2.35$. This is for a clean tank (without cylinders).

References

Arnaud G, Rey V, Touboul J, Sous D, Molin B, Gouaud F 2016 Wave propagation through vertical cylinder arrays: effect of the specific surface, submitted.

Augustin LN, Irish JI, Lynett P 2009 Laboratory and numerical studies of wave damping by emergent and near-emergent wetland vegetation, *Coastal Engineering*, **56**, 332–340.

Chen X., Chen Q., Zhan J., Liu D. 2016 Numerical simulations of wave propagation over a vegetated platform, *Coastal Engineering*, **110**, 64–75.

Faltinsen OM, Timokha AN 2009 *Sloshing*, Cambridge University Press.

Lowe RJ, Koseff JR, Monismith SG 2005 Oscillatory flow through submerged canopies: 1. Velocity structure, *J. Geophysical Res.*, **110**, C10016, doi:10.1029/2004JC002788.

Mei CC, Chan IC, Liu PLF, Huang Z, Zhang W 2011 Long waves through emergent coastal vegetation, *J. Fluid Mech.*, **687**, 461–491.

Mei CC, Chan IC, Liu PLF 2014 Waves of intermediate length through an array of vertical cylinders, *Environ Fluid Mech*, **14**, 235–261.

Molin B, Kimmoun O, Remy F, Chatjigeorgiou IK 2014, Third-order effects in wave-body interaction, *European Journal of Mechanics B/Fluids*, **47**, 132–144.

Molin B, Remy F 2013 Experimental and numerical study of the sloshing motion in a rectangular tank with a perforated screen, *J. Fluids and Structures*, **43**, 463–480.

Molin B, Remy F, Arnaud G, Rey V, Touboul J, Sous D 2016 On the dispersion equation for linear waves traveling through or over dense arrays of vertical cylinders, to appear in *Applied Ocean Research*.

Molin B, Remy F, Coudray T, Rigaud S, Mary C 2003 Etude numérique et expérimentale de la réponse à la houle d'un ensemble flotteur + cuves partiellement remplies, in *9èmes Journées de l'Hydrodynamique*, Poitiers (in French).

Molin B, Remy F, Rigaud S, de Jouette C 2002 LNG-FPSO's: frequency domain, coupled analysis of support and liquid cargo motions, in *Proc. IMAM 2002 Conf.*, Rethymno.

Sarpkaya T 2010 *Wave Forces on Offshore Structures*, Cambridge University Press.

Sarpkaya T 1986 Force on a circular cylinder in viscous oscillatory flow at low Keulegan-Carpenter numbers, *J. Fluid Mech.*, **165**, 61–71.

Sollitt CK, Cross RH 1972 Wave transmission through permeable breakwaters, in *Proc. 13th Conf. Coastal Engineering*, ASCE, New-York, N.Y., 1827–1846.

Wu W, Zhang M, Ozeren Y, Wren D 2013 Analysis of vegetation effect on waves using a vertical 2D RANS model, *J. Coastal Res.*, **29**, 383?-397.

Yu X, Chwang AT 1994 Wave motion through porous structures, *J. Engineering Mech.*, **120**, 989–1008.